International Applied Mechanics, Vol. 42, No. 12, 2006

STRESS ANALYSIS OF CIRCUMFERENTIALLY CORRUGATED HOLLOW ORTHOTROPIC CYLINDERS

Ya. M. Grigorenko and L. S. Rozhok

UDC 539.3

A problem-solving approach based on discrete Fourier series is used to analyze the stress state of corrugated orthotropic and transversely isotropic hollow cylinders

Keywords: circumferentially corrugated hollow orthotropic cylinder, stress state

Introduction. One of the main lines of development of modern engineering is the wide use of composites in various structures. Elements of such structures often have a complex form such as that of noncircular cylinders [1, 4, 15, 16].

It is of interest to study the influence of orthotropy on the stress state of circumferentially corrugated hollow cylinders subject to internal pressure.

This class of problems is treated in a three-dimensional formulation. To solve them, use is made of the variable separation method for the longitudinal coordinate, discrete Fourier series approximation for the circumferential coordinate, and the discrete-orthogonalization method for the thickness coordinate. These analytic methods and stable numerical method produce a solution with adequate accuracy [2, 7, 9, 12].

1. Consider noncircular cylinders subject to internal pressure. We will use an orthogonal curvilinear coordinate system s, ψ, and γ, where s is the circumferential coordinate; ψ is the polar angle in the cross section; and γ is the normal coordinate.

The first quadratic form of the cylinder is given by

$$dS^2 = ds^2 + A_2^2(\psi,\gamma)d\psi^2 + d\gamma^2, \tag{1}$$

where

$$A_2(\psi,\gamma) = H_2(\psi,\gamma)\omega(\psi), \qquad H_2(\psi,\gamma) = 1+\gamma/R(\psi). \tag{2}$$

The directrix of the datum surface $\gamma = \gamma_0$ is specified in the cross-sectional plane using polar coordinates:

$$\rho(\psi) = r_0 + \alpha\cos m\psi \,(0 \le \psi \le 2\pi), \tag{3}$$

ρ is the polar radius, ψ is the polar angle, r_0 is the radius of the mid-circle, α is the amplitude, and m is the number of corrugations.

Then the transformation coefficient is

$$\omega(\psi) = \sqrt{\rho^2 + \left(\frac{d\rho}{d\psi}\right)^2} = \sqrt{\left(r_0 + \alpha\cos m\psi\right)^2 + \left(\alpha m \sin m\psi\right)^2}, \tag{4}$$

and the radius of curvature of the datum surface is

S. P. Timoshenko Institute of Mechanics, National Academy of Sciences of Ukraine, Kiev. Translated from Prikladnaya Mekhanika, Vol. 42, No. 12, pp. 87–96, December, 2006. Original article submitted May 30, 2006.

$$R(\psi)=\frac{\sqrt{\left[\left(r_0+\alpha\cos m\psi\right)^2+\left(\alpha m\sin m\psi\right)^2\right]^3}}{\left(r_0+\alpha\cos m\psi\right)^2+2\left(\alpha m\sin m\psi\right)^2+\left(r_0+\alpha\cos m\psi\right)\alpha m^2\cos m\psi}. \tag{5}$$

We start with the governing equations of a three-dimensional elasticity for an orthotropic body [4–6, 10].

Let the three stress components σ_γ, $\tau_{s\gamma}$, and $\tau_{\psi\gamma}$ and the three displacement components u_γ, u_s, and u_ψ be unknown functions, i.e., we choose functions in terms of which boundary conditions on the cylinder's surfaces $\gamma_1 \le \gamma \le \gamma_2$ are formulated. After some transformations, we obtain a governing system of partial differential equations of the sixth order with variable coefficients:

$$\frac{\partial\sigma_\gamma}{\partial\gamma}=\left(c_2-1\right)\frac{1}{H_2}\frac{\partial H_2}{\partial\gamma}\sigma_\gamma-\frac{\partial\tau_{s\gamma}}{\partial s}-\frac{1}{H_2\omega}\frac{\partial\tau_{\psi\gamma}}{\partial\psi}+b_{22}\left(\frac{1}{H_2}\frac{\partial H_2}{\partial\gamma}\right)^2u_\gamma$$

$$+b_{12}\frac{1}{H_2}\frac{\partial H_2}{\partial\gamma}\frac{\partial u_s}{\partial s}+b_{22}\frac{1}{H_2^2\omega}\frac{\partial H_2}{\partial\gamma}\frac{\partial u_\psi}{\partial\psi},$$

$$\frac{\partial\tau_{s\gamma}}{\partial\gamma}=-c_1\frac{\partial\sigma_\gamma}{\partial s}-\frac{1}{H_2}\frac{\partial H_2}{\partial\gamma}\tau_{s\gamma}-b_{12}\frac{1}{H_2}\frac{\partial H_2}{\partial\gamma}\frac{\partial u_\gamma}{\partial s}-b_{11}\frac{\partial^2u_s}{\partial s^2}$$

$$-b_{66}\frac{1}{H_2\omega}\frac{\partial}{\partial\psi}\left(\frac{1}{H_2\omega}\frac{\partial u_s}{\partial\psi}\right)-\left(b_{12}+b_{66}\right)\frac{1}{H_2\omega}\frac{\partial^2u_\psi}{\partial s\partial\psi},$$

$$\frac{\partial\tau_{\psi\gamma}}{\partial\gamma}=-c_2\frac{1}{H_2\omega}\frac{\partial\sigma_\gamma}{\partial\psi}-\frac{2}{H_2}\frac{\partial H_2}{\partial\gamma}\tau_{\psi\gamma}-b_{22}\frac{1}{H_2\omega}\frac{\partial}{\partial\psi}\left(\frac{1}{H_2}\frac{\partial H_2}{\partial\gamma}u_\gamma\right)$$

$$-\left(b_{12}+b_{66}\right)\frac{1}{H_2\omega}\frac{\partial^2u_s}{\partial s\partial\psi}-b_{22}\frac{1}{H_2\omega}\frac{\partial}{\partial\psi}\left(\frac{1}{H_2\omega}\frac{\partial u_\psi}{\partial\psi}\right)-b_{66}\frac{\partial^2u_\psi}{\partial s^2},$$

$$\frac{\partial u_\gamma}{\partial\gamma}=c_4\sigma_\gamma-c_2\frac{1}{H_2}\frac{\partial H_2}{\partial\gamma}u_\gamma-c_1\frac{\partial u_s}{\partial s}-c_2\frac{1}{H_2\omega}\frac{\partial u_\psi}{\partial\psi},$$

$$\frac{\partial u_s}{\partial\gamma}=a_{55}\tau_{s\gamma}-\frac{\partial u_\gamma}{\partial s},\qquad\frac{\partial u_\psi}{\partial\gamma}=a_{44}\tau_{\psi\gamma}-\frac{1}{H_2\omega}\frac{\partial u_\gamma}{\partial\psi}+\frac{1}{H_2}\frac{\partial H_2}{\partial\gamma}u_\psi$$

$$(0\le s\le l,\ 0\le\psi\le2\pi,\ \gamma_1\le\gamma\le\gamma_2), \tag{6}$$

where for the orthotropic material [5]:

$$b_{11}=a_{22}a_{66}/\Omega,\qquad b_{12}=-a_{12}a_{66}/\Omega,\qquad b_{22}=a_{11}a_{66}/\Omega,$$

$$b_{66}=\left(a_{11}a_{22}-a_{12}^2\right)\Big/\Omega,\qquad\Omega=\left(a_{11}a_{22}-a_{12}^2\right)a_{66},$$

$$c_1=-\left(b_{11}a_{13}+b_{12}a_{23}\right),\qquad c_2=-\left(b_{12}a_{13}+b_{22}a_{23}\right),\qquad c_4=a_{33}+c_1a_{13}+c_2a_{23}, \tag{7}$$

$$a_{11}=\frac{1}{E_s},\qquad a_{12}=-\frac{\nu_{s\psi}}{E_\psi}=-\frac{\nu_{\psi s}}{E_s},\qquad a_{13}=-\frac{\nu_{s\gamma}}{E_\gamma}=-\frac{\nu_{\gamma s}}{E_s},\qquad a_{22}=\frac{1}{E_\psi},$$

$$a_{23}=-\frac{\nu_{\gamma\psi}}{E_\psi}=-\frac{\nu_{\psi\gamma}}{E_\gamma},\qquad a_{33}=\frac{1}{E_\gamma},\qquad a_{44}=\frac{1}{G_{\psi\gamma}},\qquad a_{55}=\frac{1}{G_{s\gamma}},\qquad a_{66}=\frac{1}{G_{\psi s}}, \tag{8}$$

E_s, E_ψ, and E_γ are the elastic moduli; $G_{\psi\gamma}, G_{s\gamma}$, and $G_{s\psi}$ are the shear moduli; and $\nu_{\psi\gamma}, \nu_{s\gamma}, \nu_{s\psi}$ and $\nu_{\gamma\psi}, \nu_{\gamma s}, \nu_{\psi s}$ are Poisson's ratios.

For the transversely isotropic material, we have

$$a_{11} = \frac{1}{E'}, \quad a_{12} = -\frac{\nu}{E'}, \quad a_{13} = -\frac{\nu'}{E}, \quad a_{33} = \frac{1}{E}, \quad a_{44} = \frac{1}{G'},$$

$$a_{22} = a_{11}, \quad a_{23} = a_{13}, \quad a_{55} = a_{44} a_{66} = \frac{1}{G} = \frac{2(1+\nu)}{E}. \tag{9}$$

Here $E_s = E_\psi = E, E_\gamma = E', G_{s\gamma} = G_{\psi\gamma} = G', \nu_{s\psi} = \nu, \nu_{s\gamma} = \nu_{\psi\gamma} = \nu'$, where E and E' are the elastic moduli in the coordinate a directions; G' is the shear modulus; and ν and ν' are Poisson's ratios.

2. Consider cylinders with a diaphragm perfectly rigid in its plane and flexible out of it at each of the ends:

$$\sigma_s = u_\psi = u_\gamma = 0 \quad \text{for} \quad s = 0, \; s = l. \tag{10}$$

The following boundary conditions are prescribed on the lateral surfaces:

$$\sigma_\gamma = q_\gamma^-, \quad \tau_{s\gamma} = 0, \quad \tau_{\psi\gamma} = 0 \quad \text{for} \quad \gamma = \gamma_1,$$

$$\sigma_\gamma = 0, \quad \tau_{s\gamma} = 0, \quad \tau_{\psi\gamma} = 0 \quad \text{for} \quad \gamma = \gamma_2. \tag{11}$$

The end conditions (10) reduce the dimension of the problem, i.e., enable the separation of variables with respect to the coordinate s by expanding the unknown functions and load components into Fourier series in the longitudinal direction of the cylinder. After separation of variables, we arrive at a two-dimensional boundary-value problem described by a system of partial differential equations with variable coefficients. Since the cross section is noncircular, some coefficients of the governing system of equations will depend on both coordinates ψ and γ. Therefore, to separate variables with respect to the coordinate ψ, we substitute additional functions for expressions containing products of these coefficients and unknown functions [2, 3, 10–14]. Then the governing system of differential equations becomes (the index n is omitted for simplicity)

$$\frac{\partial \sigma_\gamma}{\partial \gamma} = (c_2 - 1)\,\varphi_1^1 + \lambda_n \tau_{s\gamma} - \varphi_4^1 + b_{22}\varphi_1^5 + b_{12}\lambda_n \varphi_1^4 + b_{22}\varphi_4^3,$$

$$\frac{\partial \tau_{s\gamma}}{\partial \gamma} = -c_1 \lambda_n \sigma_\gamma - \varphi_1^2 - b_{12}\lambda_n \varphi_1^3 + b_{11}\lambda_n^2 u_s - b_{66}\varphi_6 - (b_{12} + b_{66})\,\lambda_n \varphi_4^2,$$

$$\frac{\partial \tau_{\psi\gamma}}{\partial \gamma} = -c_2 \varphi_3^1 - 2\varphi_2^1 - b_{22}\varphi_5 + (b_{12} + b_{66})\,\lambda_n \varphi_3^3 - b_{22}\varphi_7 + b_{66}\lambda_n^2 u_\psi,$$

$$\frac{\partial u_\gamma}{\partial \gamma} = c_4 \sigma_\gamma - c_2 \varphi_4^2 + c_1 \lambda_n u_s - c_2 \varphi_1^3, \quad \frac{\partial u_s}{\partial \gamma} = a_{44}\tau_{s\gamma} - \lambda_n u_\gamma, \quad \frac{\partial u_\psi}{\partial \gamma} = a_{44}\tau_{\psi\gamma} - \varphi_3^2 + \varphi_2^2, \tag{12}$$

where

$$\varphi_1^j = \frac{1}{H_2}\frac{\partial H_2}{\partial \gamma}\left\{\sigma_\gamma; \tau_{s\gamma}; u_\gamma; u_s; \frac{1}{H_2}\frac{\partial H_2}{\partial \gamma} u_\gamma\right\} \quad \left(j = \overline{1,5}\right),$$

$$\varphi_2^j = \frac{1}{H_2}\frac{\partial H_2}{\partial \gamma}\left\{\tau_{\psi\gamma}; u_\psi\right\} \quad \left(j = \overline{1,2}\right),$$

$$\varphi_3^j = \frac{1}{H_2 \omega}\left\{\frac{\partial \sigma_\gamma}{\partial \psi}; \frac{\partial u_\gamma}{\partial \psi}; \frac{\partial u_s}{\partial \psi}\right\} \quad \left(j = \overline{1,3}\right),$$

$$\varphi_4^j = \frac{1}{H_2\omega}\left\{\frac{\partial\tau_{\psi\gamma}}{\partial\psi};\frac{\partial u_\psi}{\partial\psi};\frac{1}{H_2}\frac{\partial H_2}{\partial\gamma}\frac{\partial u_\psi}{\partial\psi}\right\} \quad \left(j=\overline{1,3}\right),$$

$$\varphi_5 = \frac{1}{H_2\omega}\frac{\partial}{\partial\psi}\varphi_1^3, \quad \varphi_6 = \frac{1}{H_2\omega}\frac{\partial}{\partial\psi}\varphi_3^3, \quad \varphi_7 = \frac{1}{H_2\omega}\frac{\partial}{\partial\psi}\varphi_4^2 \tag{13}$$

with the boundary conditions

$$\sigma_\gamma = q_\gamma^-, \quad \tau_{s\gamma}=0, \quad \tau_{\psi\gamma}=0 \quad \text{for} \quad \gamma=\gamma_1,$$

$$\sigma_\gamma = 0, \quad \tau_{s\gamma}=0, \quad \tau_{\psi\gamma}=0 \quad \text{for} \quad \gamma=\gamma_2. \tag{14}$$

Let us expand all the functions in (12), the boundary conditions (14), and expressions (13) into Fourier series in ψ:

$$\widetilde{X}(\psi,\gamma) = \sum_{k=0}^{K}\widetilde{X}_k(\gamma)\cos k\psi, \quad \widetilde{Y}(\psi,\gamma) = \sum_{k=1}^{K}\widetilde{Y}_k(\gamma)\sin k\psi,$$

$$\widetilde{X} = \left\{\sigma_\gamma,\tau_{s\gamma},u_\gamma,u_s,\varphi_1^j,\varphi_4^j,\varphi_6,q_\gamma\right\}, \quad \widetilde{Y} = \left\{\tau_{\psi\gamma},u_\psi,\varphi_2^j,\varphi_3^j,\varphi_5,\varphi_7\right\}. \tag{15}$$

Substituting series (15) into the governing system of equations (12) and boundary conditions (14) and separating variables, we arrive at a system of ordinary differential equations for each term k:

$$\frac{d\sigma_{\gamma,k}}{d\gamma} = (c_2-1)\varphi_{1,k}^1 + \lambda_n\tau_{s\gamma,k} - \varphi_{4,k}^1 + b_{22}\varphi_{1,k}^5 + b_{12}\lambda_n\varphi_{1,k}^4 + b_{22}\varphi_{4,k}^3,$$

$$\frac{d\tau_{s\gamma,k}}{d\gamma} = -c_1\lambda_n\sigma_{\gamma,k} - \varphi_{1,k}^2 + b_{12}\lambda_n\varphi_{1,k}^3 + b_{11}\lambda_n^2u_{s,k} - b_{66}\varphi_{6,k} - (b_{12}+b_{66})\lambda_n\varphi_{4,k}^2,$$

$$\frac{d\tau_{\psi\gamma,k}}{d\gamma} = -c_2\varphi_{3,k}^1 - 2\varphi_{2,k}^1 - b_{22}\varphi_{5,k} + (b_{12}+b_{66})\lambda_n\varphi_{3,k}^3 - b_{22}\varphi_{7,k} + b_{66}\lambda_n^2u_{\psi,k},$$

$$\frac{du_{\gamma,k}}{d\gamma} = c_4\sigma_{\gamma,k} - c_2\varphi_{4,k}^2 + c_1\lambda_nu_{s,k} - c_2\varphi_{1,k}^3, \qquad \frac{du_{s,k}}{d\gamma} = a_{44}\tau_{s\gamma,k} - \lambda_nu_{\gamma,k},$$

$$\frac{du_{\psi,k}}{d\gamma} = a_{44}\tau_{\psi\gamma,k} - \varphi_{3,k}^2 + \varphi_{2,k}^2 \qquad \left(k=\overline{0,K}\right) \tag{16}$$

with the boundary conditions

$$\gamma=\gamma_1: \ \sigma_{\gamma,k} = q_{\gamma,k}^-, \quad \tau_{s\gamma,k}=0, \quad \tau_{\psi\gamma,k}=0,$$

$$\gamma=\gamma_2: \ \sigma_{\gamma,k}=0, \quad \tau_{s\gamma,k}=0, \quad \tau_{\psi\gamma,k}=0. \tag{17}$$

3. The boundary-value problem (16), (17) is solved by the stable discrete-orthogonalization method [1]. During the integration, the additional functions (represented as tables) are approximated by discrete Fourier series to determine their amplitude values [7, 8]. As the number of points at which the additional functions are calculated increases, the discrete Fourier series tends to the ordinary Fourier series, which allows reaching the prescribed accuracy [2, 7, 9, 12].

Let us use the approach outlined above to analyze the dependence of the stress state of circumferentially corrugated hollow orthotropic cylinders subjected to internal pressure $q=-q_0\sin(\pi s/l)$ ($q_0=\text{const}$) on the thickness of the wall, the number and amplitude of corrugations, and the parameters of orthotropy.

4. Input data: the radius of the mid-surface $r_0=60$, the length of the cylinder $L=40$, the thickness of its wall $h=3, 4$, the number of corrugations $m=4, 8$, the amplitude of corrugation $\alpha=2, 4, 6, 8$. If the cylinders are orthotropic, then we have the

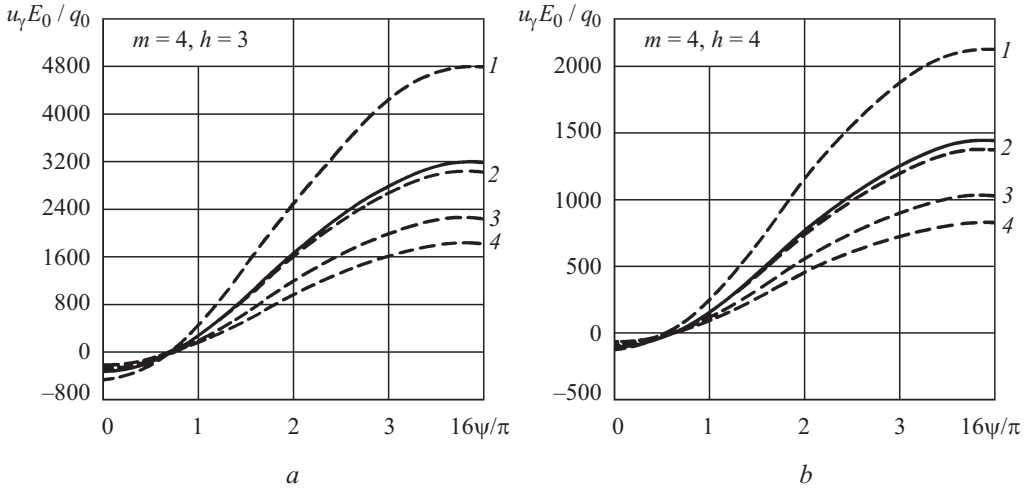

a *b*

Fig. 1

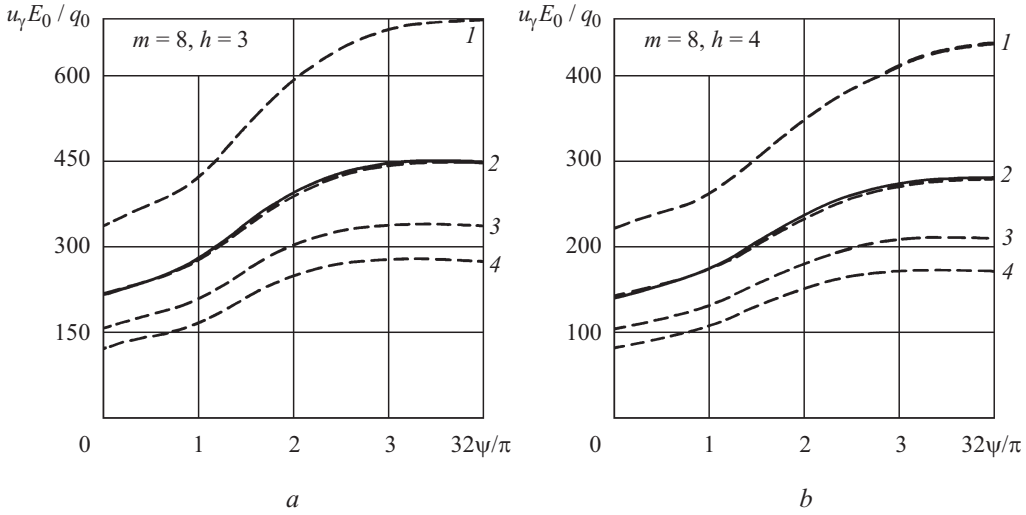

a *b*

Fig. 2

following mechanical parameters [5]: $E_s = 3.68E_0$, $E_\psi = 2.68E_0$, $E_\gamma = 1.1E_0$, $\nu_{s\psi} = 0.105$, $\nu_{s\gamma} = 0.405$, $\nu_{\psi\gamma} = 0.431$, $G_{s\psi} = 0.5E_0$, $G_{s\gamma} = 0.45E_0$, $G_{\psi\gamma} = 0.41E_0$. If the cylinders are transversely isotropic, then these parameters are $E_s = E_\psi = 1.68E_0, 2.68E_0, 3.68E_0, 4.68E_0, \nu_{s\psi} = 0.105, \nu_{s\gamma} = \nu_{\psi\gamma} = 0.405, G_{s\gamma} = G_{\psi\gamma} = 0.45E_0$.

Table 1 compares the displacements and stresses in orthotropic and transversely isotropic cylinders.

Figure 1 shows the distribution of the normal displacement u_γ for $m = 4$, $\alpha = 4$, $h = 3$, 4, and $0 \le \psi \le \pi / 4$ in the section $s = L / 2, \gamma = \gamma_0$ for an orthotropic cylinder (solid line) and a transversely isotropic cylinder (dashed lines) with E_s = 1.28 (case *1*), E_s = 2.28 (case *2*), E_s = 3.28 (case *3*), and E_s = 4.28 (case *4*).

It can be seen from Fig. 1*a* that the displacements u_γ at the crest of corrugation are opposite to the acting load. At the trough of corrugation, the deflection of the orthotropic cylinder is close to that of the transversely isotropic cylinder in case *2*, is less by a factor of 1.5 than in case *1*, is 1.39 of the value in case *3*, and is 1.79 of the value in case *4*.

Figure 1*b* demonstrates that the deflections in cylinders with thickness $h = 4$ are almost half that in cylinders with $h = 3$, the distribution patterns of displacements u_γ being similar at the crest of corrugation and close at the trough of corrugation.

Figure 2 shows the deflection in cylinders with $m = 8$ for the same parameters and $0 \le \psi \le \pi / 8$. It is significant (Fig. 2*a*) that the deflections of the orthotropic and transversely isotropic (case *2*) cylinders practically coincide, and in cases *1*, *3*, and *4* the deflections are in almost the same ratio as in the cylinders with m = 4. The pattern shown in Fig. 2*b* is similar.

Figure 3 shows the distribution of stresses σ_ψ over the outer (II) and inner (I) lateral surfaces of the orthotropic (solid line) and transversely isotropic (case *2*, dashed line) cylinders with m =4, 8, $\alpha = 4$. Curves *1* and *2* correspond to h = 3 and h = 4. It

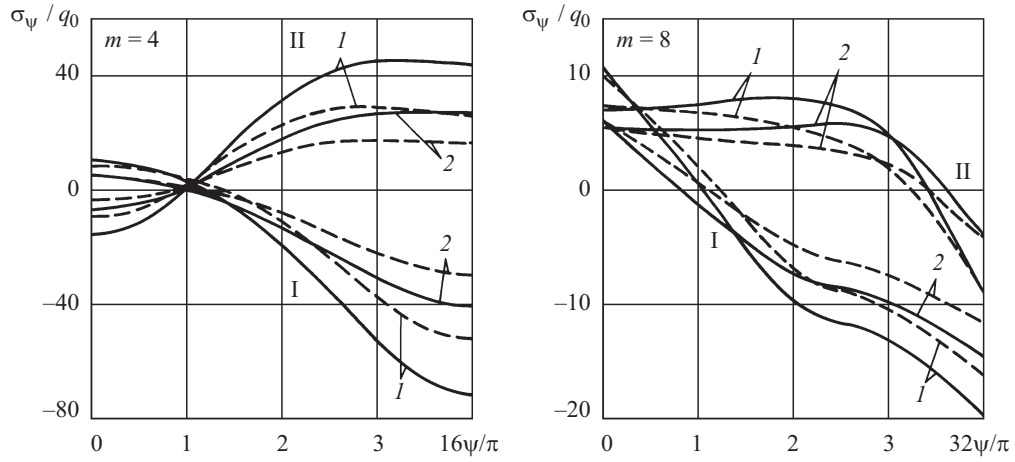

a *b*

Fig. 3

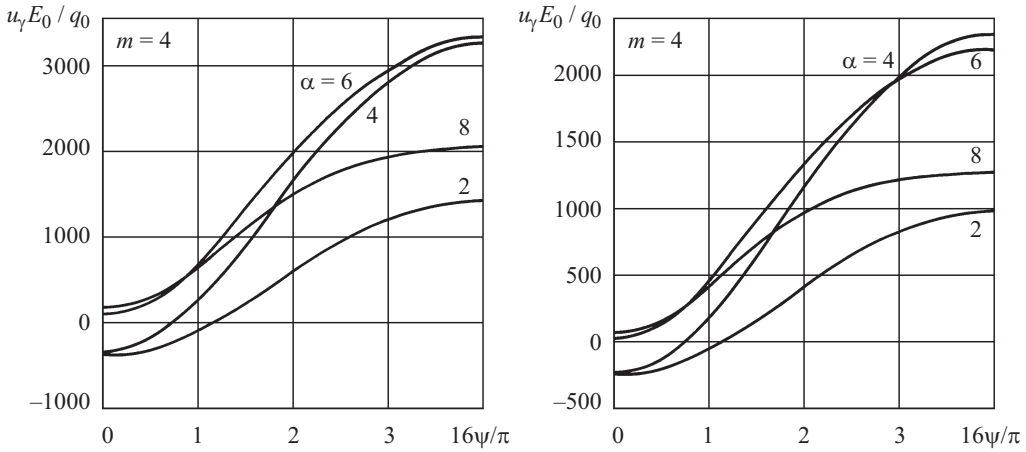

a *b*

Fig. 4

can be seen that the stresses σ_ψ strongly depend, both quantitatively and qualitatively, on the number of corrugations. The stresses in the transversely isotropic cylinder with $m = 4$ and $m = 8$ differ insignificantly from those in the orthotropic cylinder.

Table 1 summarizes the stresses σ_ψ on the outer and inner surfaces of the orthotropic and transversely isotropic cylinders, in the section $s = L/2$ on the interval $0 \le \psi \le \pi/4$ for $m = 4$ and on the interval $0 \le \psi \le \pi/8$ for $m = 8$ when $\alpha = 4$, $h = 3$, 4. It can be seen that the stresses do not depend significantly on E_s for both $h = 3$ and $h = 4$ and for $m = 4$ and $m = 8$.

Figure 4 shows the distribution of the normal displacement u_γ of the mid-surface of the orthotropic (Fig. 4*a*) and transversely isotropic (case *3*, Fig. 4*b*) cylinders for different values of $\alpha = 2, 4, 6, 8$ in the section $s = L/2$.

It can be seen from Fig. 4*a* that for $\alpha = 2, 4, 6$, i.e., as the convexity of corrugation increases, the deflection mainly increases too, which is indicative of greater resistance to the applied load. For $\alpha = 8$, the pattern changes with distance from the crest of corrugation, which indicates the influence of the corrugation form on the resistance to load. Figure 4*b* demonstrates the influence of the material characteristics on the deflections of the transversely isotropic cylinder.

Figure 5 show how the number of corrugations influences the deflection u_γ and its circumferential distribution. Here the minimum amplitude ($\alpha = 2$) corresponds to the maximum deflection, and the maximum amplitude ($\alpha = 8$) to the minimum deflection. This can apparently be attributed to the fact that a cylinder with more corrugations is more rigid. While the deflections of the cylinders with $m = 4$ and $m = 8$ are almost equal when $\alpha = 2$, the difference in the number of corrugations is noticeable for other values of the amplitude. There is also some difference between the deflections of orthotropic and transversely isotropic cylinders (Fig. 5).

TABLE 1

h	γ	σ_ψ / q_0										
		$m = 4$						$m = 8$				
		ψ	0	$\pi/16$	$\pi/8$	$3\pi/16$	$\pi/4$	0	$\pi/16$	$\pi/8$	$3\pi/16$	$\pi/4$
3	γ_1	ort	10.14	3.43	–19.20	–53.42	–71.79	10.68	0.45	–9.75	–13.10	–19.55
		1	8.44	4.33	–11.79	–38.23	–52.60	10.17	2.09	–6.65	–10.51	–15.84
		2	7.78	3.77	–12.23	–38.74	–53.19	9.87	1.79	–7.12	–11.15	–16.56
		3	7.12	3.21	–12.66	–39.24	–53.78	9.55	1.48	–7.58	–11.76	–17.23
		4	6.47	2.66	–13.08	–39.73	–54.37	9.23	1.16	–8.02	–12.35	–17.88
	γ_2	ort	–16.86	0.72	31.99	45.51	44.93	7.04	7.50	8.15	5.14	–8.57
		1	–10.15	2.43	23.14	29.06	26.74	7.30	6.72	5.50	1.95	–8.44
		2	–10.24	2.50	23.37	29.20	26.77	7.52	6.99	5.68	1.99	–8.54
		3	–10.33	2.56	23.60	29.34	26.80	7.72	7.24	5.83	2.01	–8.65
		4	–10.43	2.62	23.83	29.48	26.83	7.89	7.46	5.96	2.03	–8.77
4	γ_1	ort	4.94	0.31	–13.31	–31.55	–40.86	5.96	–1.11	–7.25	–9.78	–14.40
		1	4.54	1.42	–8.49	–22.50	–29.72	6.01	0.49	–4.80	–7.59	–11.38
		2	3.96	0.92	–8.90	–22.98	–30.26	5.66	0.12	–5.30	–8.16	–11.99
		3	3.40	0.42	–9.31	–23.44	–30.80	5.31	–0.25	–5.77	–8.71	–12.56
		4	2.83	–0.07	–9.71	–23.90	–31.33	4.96	–0.60	–6.21	–9.22	–13.10
	γ_2	ort	–16.86	0.72	31.99	45.51	44.93	5.38	5.22	5.73	4.86	–3.70
		1	–10.15	2.43	23.14	29.06	26.74	5.35	4.58	3.79	2.34	–4.08
		2	–10.24	2.50	23.37	29.20	26.77	5.54	4.83	3.97	2.38	–4.20
		3	–10.33	2.56	23.60	29.34	26.80	5.71	5.05	4.13	2.40	–4.32
		4	–10.43	2.62	23.83	29.48	26.83	5.86	5.24	4.26	2.43	–4.43

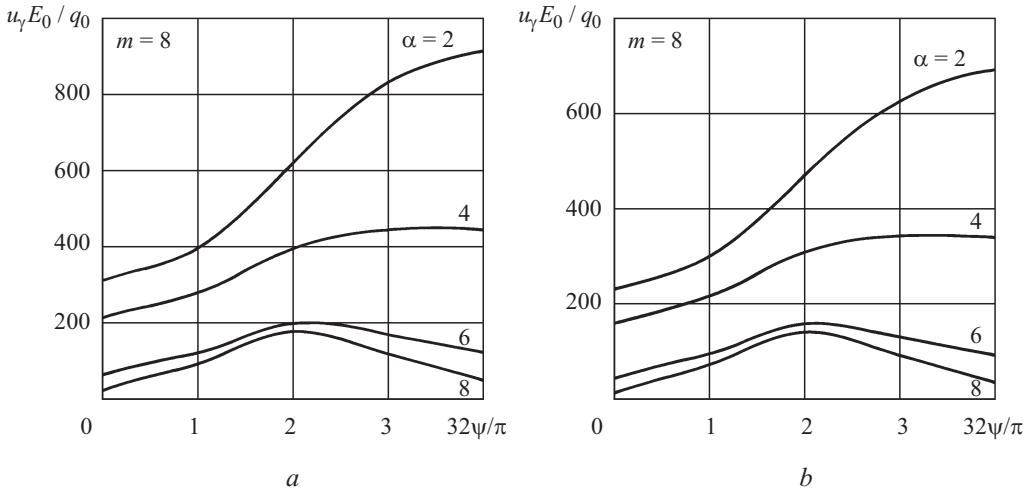

a *b*

Fig. 5

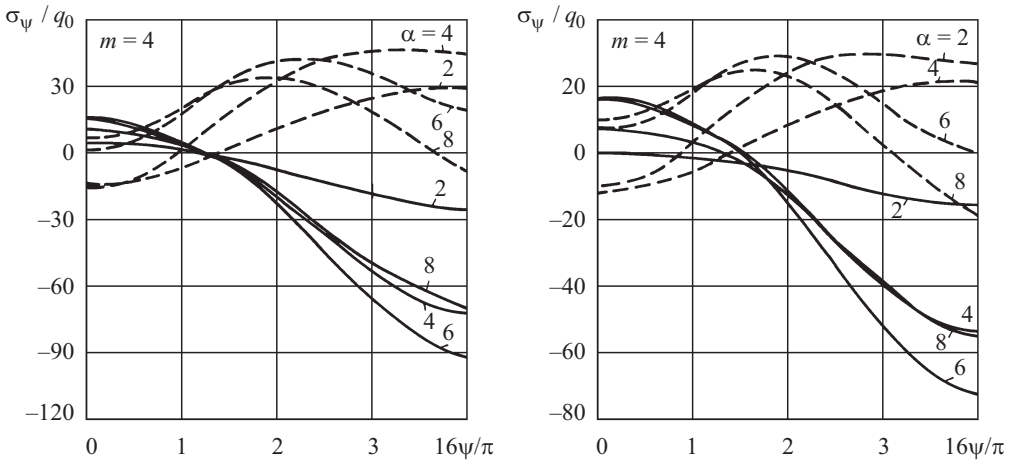

a *b*

Fig. 6

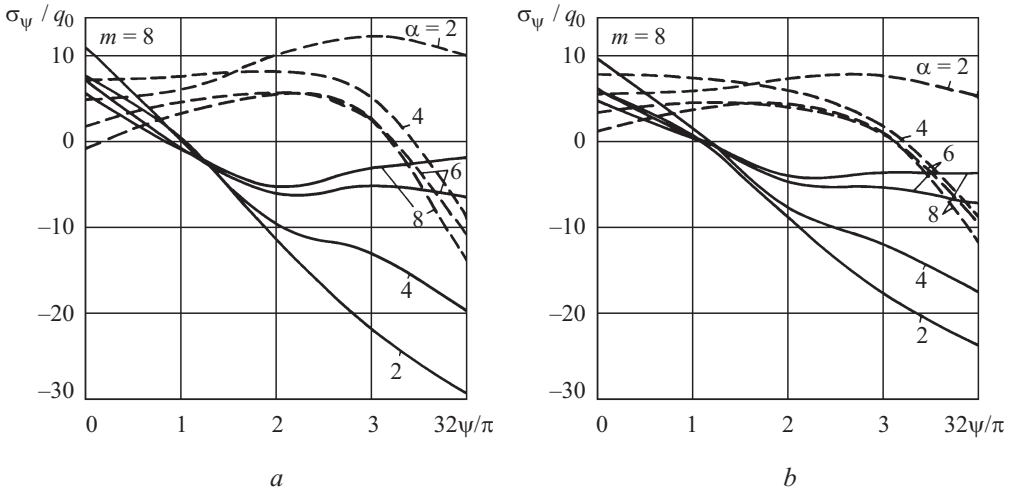

a *b*

Fig. 7

Figure 6 shows the distribution of the stresses σ_ψ on the outer (dashed line) and inner (solid line) surfaces of the orthotropic (Fig. 6*a*) and transversely isotropic (Fig. 6*b*) cylinders for $\alpha = 2, 4, 6, 8$, and $m = 4$. The stresses in the transversely isotropic cylinder are less by a factor of approximately 1.5 than in the orthotropic cylinder. The stress distribution over the inner surface is more smooth for $\alpha = 2$ than for $\alpha = 4, 6, 8$. The stress distribution over the outer surface of the cylinder is more smooth when $\alpha = 2, 4$. Similar curves for the stress σ_ψ in cylinders with $m = 8$ are shown in Fig. 7. It can well be seen how the corrugation amplitude α affects the stress distribution pattern (the stresses decrease because of the increasing stiffness of the cylinders).

REFERENCES

1. Ya. M. Grigorenko, A. T. Vasilenko, I. G. Emel'yanov, et al., *Statics of Structural Members*, Vol. 8 of the 12-volume series *Mechanics of Composite Materials* [in Russian], A.S.K., Kyiv (1999).
2. Ya. M. Grigorenko and L. S. Rozhok, "Applying discrete Fourier series to solve static boundary-value problems for noncanonical elastic bodies," *Mat. Metody Fiz.-Mekh. Polya*, **48**, No. 2, 78–100 (2005).
3. Ya. M. Grigorenko and A. M. Timonin, "An approach to the numerical solution of two-dimensional problems of plate and shell theory with variable parameters," *Int. Appl. Mech*., **23**, No. 6, 557–563 (1987).
4. A. N. Guz and Yu. N. Nemish, *Statics of Noncanonical Elastic Bodies*, Vol. 2 of the six-volume series *Three-Dimensional Problems of Elasticity and Plasticity* [in Russian], Naukova Dumka, Kyiv (1984).
5. S. G. Lekhnitskii, *Anisotropic Elasticity Theory* [in Russian], Nauka, Moscow (1977).
6. S. P. Timoshenko, *A Course on the Theory of Elasticity* [in Russian], Naukova Dumka, Kyiv (1972).
7. G. M. Fikhtengol'ts, *A Course of Differential and Integral Calculus* [in Russian], Vol. 3, Nauka, Moscow (1949).
8. R. W. Hamming, *Numerical Methods for Scientists and Engineers*, McGraw-Hill, New York (1962).
9. Ya. M. Grigorenko and L. S. Rozhok, "Discrete Fourier-series method in problems of bending of variable-thickness rectangular plates," *J. Eng. Math*., **46**, No. 3–4, 269–280 (2003).
10. Ya. M. Grigorenko and L. S. Rozhok, "On one approach to the solution of stress problems for noncircular hollow cylinders," *Int. Appl. Mech*., **38**, No. 5, 562–573 (2002).
11. Ya. M. Grigorenko and L. S. Rozhok, "Stress solution for transversely isotropic corrugated hollow cylinders," *Int. Appl. Mech*., **41**, No. 3, 277–282 (2005).
12. Ya. M. Grigorenko and V. A. Tsibul'nik, "Application of discrete Fourier series in the stress analysis of cylindrical shells of variable thickness with arbitrary end condition," *Int. Appl. Mech*., **41**, No. 6, 657–665 (2005).
13. Ya. M. Grigorenko and V. A. Tsibul'nik, "On a discrete Fourier series solution to static problem for conical shells of circumferentially varying thickness," *Int. Appl. Mech*., **41**, No. 9, 976–987 (2005).
14. Ya. M. Grigorenko and V. A. Tsibul'nik, "Stress–strain analysis of conical shells with different boundary conditions and thickness varying in two directions at constant mass," *Int. Appl. Mech*., **42**, No. 3, 308–317 (2006).
15. V. G. Piskunov and A. O. Rasskazov, "Evolution of the theory of laminated plates and shells," *Int. Appl. Mech*., **38**, No. 2, 135–166 (2002).
16. K. P. Soldatos, "Mechanics of cylindrical shells with noncircular cross-section: A survey," *Appl. Mech. Rev*., **52**, No. 8, 237–274 (1999).